Mathematical analysis of SOFC based on co-ionic conducting electrolyte

Keqing Zheng, Meng Ni*, Qiong Sun, Li-yin Shen

Building Energy Research Group, Department of Building and Real Estate,
The Hong Kong Polytechnic University, Hung Hom, Kowloon, Hong Kong, China

Abstract:

In co-ionic conducting solid oxide fuel cell (SOFC), both oxygen ion (O^{2-}) and proton (H^{+}) can transport through the electrolyte, generating steam in both the anode and cathode. Thus the mass transport phenomenon in the electrodes is quite different from that in conventional SOFC with oxygen ion conducting electrolyte (O-SOFC) or with proton conducting electrolyte (H-SOFC). The generation of steam in both electrodes also affects the concentration overpotential loss and further the SOFC performance. However, no detailed modeling study on SOFCs with co-ionic electrolyte has been reported yet. In this paper, a new mathematical model for SOFC based on co-ionic electrolyte is developed to predict its actual performance considering three major kinds of overpotentials. Ohm's law and the Butler-volmer formula are used to model the ion conduction and electrochemical reactions, respectively. The Dusty Gas Model (DGM) is employed to simulate the mass transport processes in the porous electrodes. Parametric simulations are performed to investigate the effects of proton transfer number (t_H) and current density (j_{total}) on the cell performance. It's interesting to find that the co-ionic conducting SOFC could perform better than O-SOFC and H-SOFC by choosing an appropriate proton transfer number. In addition, the co-ionic SOFC shows smaller difference between the anode and cathode concentration overpotentials than O-SOFC and H-SOFC at certain t_H values. The results could help material selection for enhancing SOFC performance.

Keywords: Co-ionic electrolyte, Proton transport number, Concentration overpotential, Mass transport, Model.

* Corresponding author. Tel: (852) 2766 4152; Fax: (852) 2764 5131;
Email: bsmengni@polyu.edu.hk (Meng Ni)

Solid oxide fuel cell (SOFC) is an electrochemical device which can convert chemical energy of a fuel into electrical energy directly with high efficiency and fuel flexibility. SOFC mainly consists of three components: anode and cathode provide sites for electrochemical half-reactions, while electrolyte functions as an ion transport medium between the electrodes. According to the type of ions (oxygen ions or protons) transporting in the electrolyte, SOFC can be classified to 2 kinds: oxygen ion conducting SOFC (O-SOFC) and proton conducting SOFC (H-SOFC). Although O-SOFC is traditionally used, previous research indicated that H-SOFC exhibited potentially higher efficiency than O-SOFC [1]. However, it's also reported that most proton conducting oxides show both oxygen ion and proton conductivity, which are called as "co-ionic" oxide [2-4].

Different from O-SOFC and H-SOFC, steam is generated at both anode and cathode in co-ionic conducting SOFC, leading to a different mass distribution in both electrodes. As a result, the concentration overpotentials in co-ionic conducting SOFC are essentially different from those in O-SOFC and H-SOFC. It is expected that the co-ionic effect in SOFC might lower down the electrode polarization [5]. However, previous modeling studies on co-ionic conducting SOFC are limited: Huang et al [6] derived the theoretical open-circuit voltage for SOFC with hybrid conducting (oxygen ion, proton and electron) electrolyte based on defect chemistry; Bavarian et al [7] and Demin et al [8] developed models to predict the performance of SOFCs with co-ionic conducting electrolytes. In Demin's study, the proton transfer number was assumed to be 0.5 while in Bavarian's study, $BaCe_{1-x}Sm_xO_{3-\alpha}$ was used as the co-ionic conducting electrolyte. No detailed modeling study has been performed to predict the co-ionic SOFC performance considering various overpotential losses and examine the effect of proton transfer number.

In this paper, a new mathematical model of SOFC based on co-ionic conducting electrolyte is developed to predict its actual performance. The dusty gas model (DGM),

Ohm's law and the Butler-volmer formula are used to describe the gas transport in pores, ion conduction in the electrolyte, and electrochemical reaction kinetics, respectively. Proton transfer number (t_H) defined as the ratio of proton conductivity to total conductivity is used as an indicator of proton conductivity [8-9]. Since the co-ionic property mainly affects mass transfer in both anode and cathode when total conductivity is fixed, the effect of t_H on concentration overpotentials are investigated. Parametric simulations are performed for anode-supported, electrolyte-supported and cathode-supported SOFCs at various operating voltages to examine the co-ionic effect.

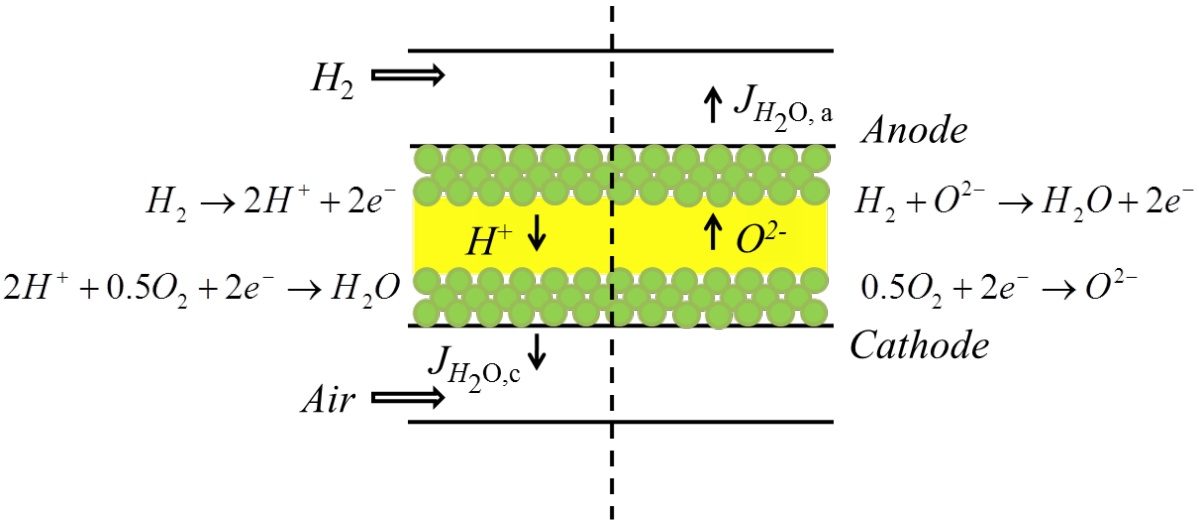

Fig. 1 Working mechanism of SOFC based on co-ionic conducting electrolyte

2. The model

2.1. Model development

Fig. 1 shows the working mechanism of SOFC based on co-ionic conducting electrolyte. Hydrogen is fed as fuel and air is used as oxidant. Electrochemical reactions are assumed to occur at the electrode-electrolyte interface only, which is valid as the reaction zone is usually very small compared with the thickness of the electrodes. Since both $O^{2-}$and H^+ can be transported through electrolyte, half-reactions evolved in electrodes are:

Anode:

$$H_2 \rightarrow 2H^+ + 2e^- \quad (1)$$

$$H_2 + O^{2-} \rightarrow H_2O + 2e^- \quad (2)$$

Cathode:

$$2H^+ + 0.5O_2 + 2e^- \rightarrow H_2O \quad (3)$$

$$0.5O_2 + 2e^- \rightarrow O^{2-} \quad (4)$$

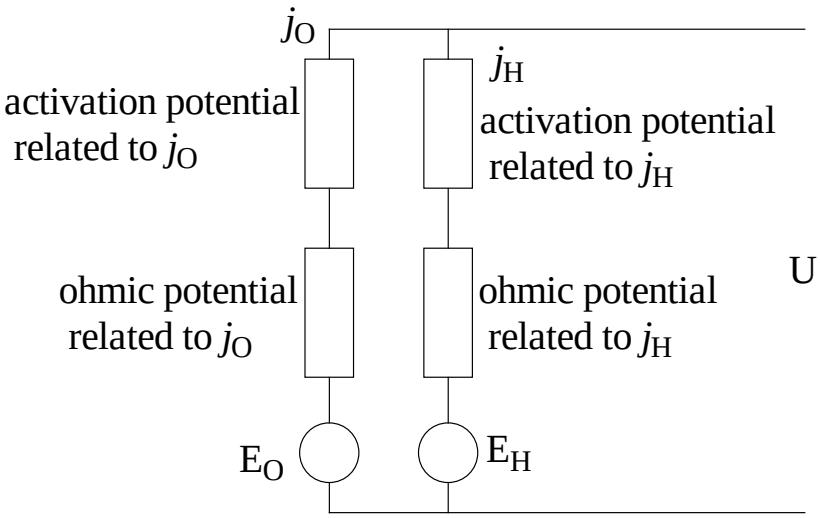

Fig. 2 Equivalent circuit diagram of co-ionic SOFC

The equivalent circuit diagram of co-ionic SOFC considering overpotential losses is shown in Fig.2. E_H and E_O represent the electromotive force caused by H^+ and O^{2-} conduction respectively. According to fuel cell thermodynamics, E_H and E_O could be described as [10]:

$$E_H = E_T - \frac{RT}{2F}\ln\left(\frac{P_{H2O,r,c}}{P_{H2,r}P_{O2,r}^{0.5}}\right) \quad (5)$$

$$E_O = E_T - \frac{RT}{2F}\ln\left(\frac{P_{H2O,r,a}}{P_{H2,r}P_{O2,r}^{0.5}}\right) \quad (6)$$

$$E_T = 1.253 - 0.00024516T \quad (7)$$

where, $P_{H2O,r,c}$ represents partial pressure of water in cathode reaction site; $P_{H2O,r,a}$ represents partial pressure of water in anode reaction site; $P_{H2,r}$ represents partial pressure of hydrogen in anode reaction site; $P_{O2,r}$ represents partial pressure of oxygen in cathode reaction site. *R*,

F and *T* refer to ideal gas constant (8.314 J mol^{-1} K^{-1}), Faraday constant (96485 C mol^{-1}) and operating temperature (K). It is noted that the concentration overpotentials are implicitly included in Eqs. (5) and (6), as the partial pressure of gas species at the reaction sites are used.

In operation, the voltage of the cell decreases due to various concentration losses. As the concentration losses have been included in the equilibrium voltages (Eqs. 5 and 6), the operating voltage *U* can be calculated as the equilibrium voltage *E* subtracted by the ohmic and activation overpotentials.

$$U = E - \eta_{act,a} - \eta_{act,c} - \eta_{ohmic} \tag{8}$$

Activation overpotential can be determined by the Butler-Volmer equation[10]:

$$\eta_{act,i} = \frac{RT}{F} ln\left(\frac{j}{2j_{o,i}} + \sqrt{\left(\frac{j}{2j_{o,i}}\right)^2 + 1}\right) \quad i = a, c \tag{9}$$

where j_0 is the exchange current density measuring the electrochemical activity of the electrode.

Ohmic overpotential can be determined by the Ohm's law:

$$\eta_{ohmic} = j\frac{L}{\sigma} \tag{10}$$

where *L* is the thickness of the electrolyte (m), σ is the ionic conductivity (S.m^{-1}). It is noted that, in Eqs. (9) and (10), *j* is the current density (associated with oxygen ion conduction or proton conduction, (A.m^{-2})).

Although concentration overpotentials are included in Eqs. (5) and (6), they can be determined separately in order to examine the effects of proton transfer number on concentration overpotential as:

$$\eta_{conc,a} = \frac{RT}{2F} ln\left(\frac{P_{H2O,TPB,a} P_{H2}}{P_{H2O,a} P_{H2,TPB}}\right) \tag{11}$$

$$\eta_{conc,c} = \frac{RT}{2F} ln\left(\frac{P_{H2O,TPB,c} P_{O2}^{0.5}}{P_{H2O,c} P_{O2,TPB}^{0.5}}\right) \tag{12}$$

The partial pressure of gas species at the electrode surface are specified as input parameters. Partial pressures at the reaction sites can be determined by DGM (more details can refer to [11-13]),

$$\frac{N_i}{D_{i,k}^{eff}} + \sum_{l=1,l\neq i}^{n} \frac{y_l N_i - y_i N_l}{D_{il}^{eff}} = -\frac{P}{RT}\frac{dy_i}{dz} \tag{13}$$

$$D_{i,k}^{eff} = \frac{\xi}{\varepsilon}\frac{2}{3} r \sqrt{\frac{8RT}{\pi M_i}} \tag{14}$$

$$D_{i,l}^{eff} = \frac{\xi}{\varepsilon}\frac{0.00267 T^{3/2}}{p M_{i,l}^{1/2} \sigma_{i,l}^{2} \Omega_D} \tag{15}$$

where,

N_i and y_i represent mass transport rate and molar fraction of species *i*;

$D_{i,k}^{eff}$ represents the effective Knudsen diffusion coefficient of gas species *i;*

D_{il}^{eff} represents the effective binary diffusion coefficient of species *i* and *l.*

It should be noted that, in steady state, the mass transport rates (flux) of steam in anode ($N_{H2O,a}$) and cathode ($N_{H2O,c}$) are governed separately by corresponding current density j_H and j_O, while the mass transport rates of N_{H2} and N_{O2} are codetermined by j_H and j_O, that is,

$$N_{H2} = \frac{j_O + j_H}{2F} \tag{16}$$

$$N_{O2} = \frac{j_O + j_H}{4F} \tag{17}$$

$$N_{H2O,a} = -\frac{j_O}{2F} \tag{18}$$

$$N_{H2O,c} = -\frac{j_H}{2F} \tag{19}$$

2.2. Calculation procedure

The calculation procedure is shown in Appendix.1: First, an output voltage *U* is specified; then j_H and j_O are assumed and used to calculate partial pressures of gas species

($P_{H2O,r,c}$, $P_{H2O,r,a}$, $P_{H2,r}$, $P_{O2,r}$) at reaction sites using Eq. (13). After that, E_H and E_O are obtained using Eq. (5) and Eq. (6). Activation overpotentials ($\eta_{H,act,a}$, $\eta_{H,act,c}$, $\eta_{O,act,a}$, $\eta_{O,act,c}$) and ohmic overpotentials ($\eta_{H,ohmic}$, $\eta_{O,ohmic}$) caused by O^{2-} conducting and H^+ conducting are calculated with j_O and j_H separately (using Eq. (9) and Eq. (10)). New obtained output voltages U_H' and U_O' using Eq. (8) are compared with previous given U to determine the calculation loop terminal or not. Computation is repeated until converged results are achieved.

For model validation, an H-SOFC performance analysis is conducted by setting $t_H = 1$ in present procedure. Input parameters are adjusted to fit the experimental conditions and are listed in Table 1. The calculated results agree well with the experimental data [14].

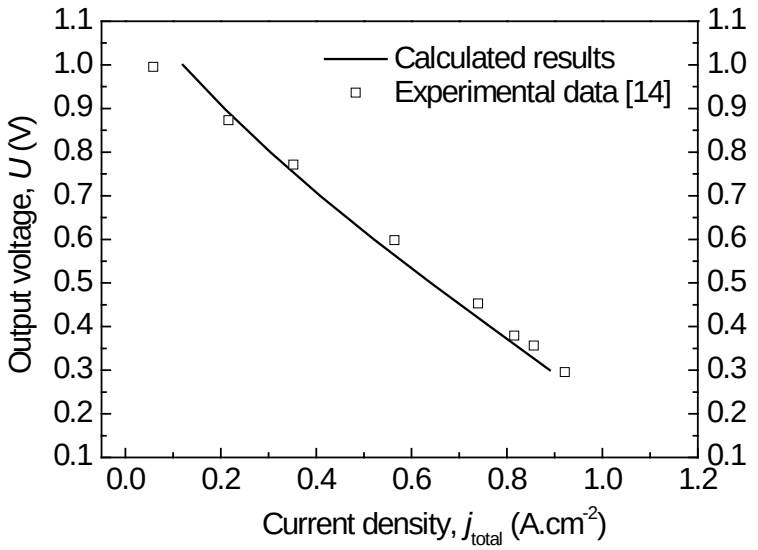

Fig. 3 Comparison between simulation results and experimental data [14] for H-SOFC

Table.1 Parameters used in model validation

Parameter	Value	Unit
Operating temperature,T	973	K
Operating pressure,P	10^5	Pa
Anode thickness, L_a	650	μm
Electrolyte thickness, L_e	50	μm

Cathode thickness,L_c	35	μm
Porosity, θ_p	0.4	
Tortuosity, τ	5	
Conductivity, σ	0.938	S m^{-1}
Average pore radius, r_p	0.5	μm
Universal gas constant, R	8.314	J mol^{-1} K^{-1}
Faraday constant, F	96485	C mol^{-1}
Exchange current density in anode, $j_{0,a}$	3000	A m^{-2}
Exchange current density in cathode, $j_{0,c}$	1000	A m^{-2}
Gas molar ratio in anode channel	H_2:H_2O=0.99:0.01	
Gas molar ratio in cathode channel	O_2:H_2O=0.97:0.03	

3. Results and discussion

In this section, the co-ionic effect on SOFC actual performance and concentration overpotentials are presented and analyzed. Simulations are conducted at an operating temperature of 1073K and a total conductivity of 3.86 S.m^{-1} for the electrolyte (conductivity of $BaCeSmO_3$, a typical co-ionic oxide) [5]. With the given total conductivity, the proton transfer number (t_H) is defined to be the ratio of proton conductivity to the total conductivity and varied in the present study. Three different supporting structures are considered: anode-supported, electrolyte-supported and cathode-supported. Gas molar ratio at the anode surface is H_2:H_2O=0.973:0.027, while at the cathode surface is O_2:N_2:H_2O=0.20:0.79:0.01 in operating condition 1 (to approximate air supply) and O_2:H_2O=0.973:0.027 in operating condition 2 (to approximate pure oxygen supply). Other parameters different from those used in model validation are summarized in Table 2. It should be noted that due to lack of solid experimental data on the exchange current densities related to j_H and j_O, it's considered

that the different transfer numbers do not affect the exchange current densities. Thus the present paper focused on the co-ionic effect on the concentration overpotentials.

Table 2 Parameters used in simulation of co-ionic conducting SOFC

Parameter	Value	Unit
Operating temperature, T	1073	K
Thickness of anode/electrolyte/cathode		μm
Anode-supported	500/50/50	
Cathode-supported	50/50/500	
Electrolyte-supported	50/500/50	
Tortuosity, τ	3	
Conductivity, σ	3.86	S m^{-1}
Exchange current density in anode, $J_{0,a}$	4000	A m^{-2}
Exchange current density in cathode, $J_{0,c}$	2000	A m^{-2}

3.1. Effect of co-ionic property on SOFC actual performance

Fig. 4 shows the actual performance of anode-supported SOFC in operating condition 1 (O_2:N_2:H_2O = 0.20:0.79:0.01 at the cathode surface). It is interesting to find that the co-ionic conducting SOFC with t_H = 0.5 performs better than both O-SOFC (t_H = 0) and H-SOFC (t_H = 1). However, when SOFC works in operating condition 2 (O_2:H_2O = 0.973:0.027 at the cathode surface), the performance of co-ionic conducting SOFC is significantly higher than O-SOFC but lower than H-SOFC (Fig. 5). From Fig. 4 and Fig. 5, it can be seen that H-SOFC perform better than O-SOFC when anode-supported structure is used, which agrees with the previous studies [15]. In comparison, O-SOFC performs better than H-SOFC when cathode-supported structure is used (Fig. 6). The performance of co-ionic conducting SOFC (t_H = 0.5 in the present case) with cathode-supported structure is between that of the O-SOFC

and H-SOFC. Fig. 7 shows that O-SOFC and H-SOFC have similar performance with electrolyte-supported structure, while co-ionic conducting SOFC (when t_H = 0.5) exhibits much better performance.

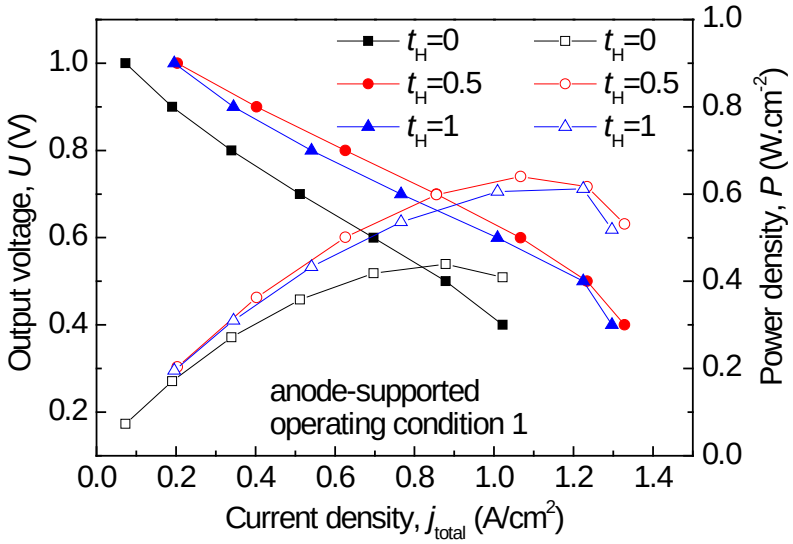

Fig. 4 Performance simulation of anode-supported SOFC in operating condition 1

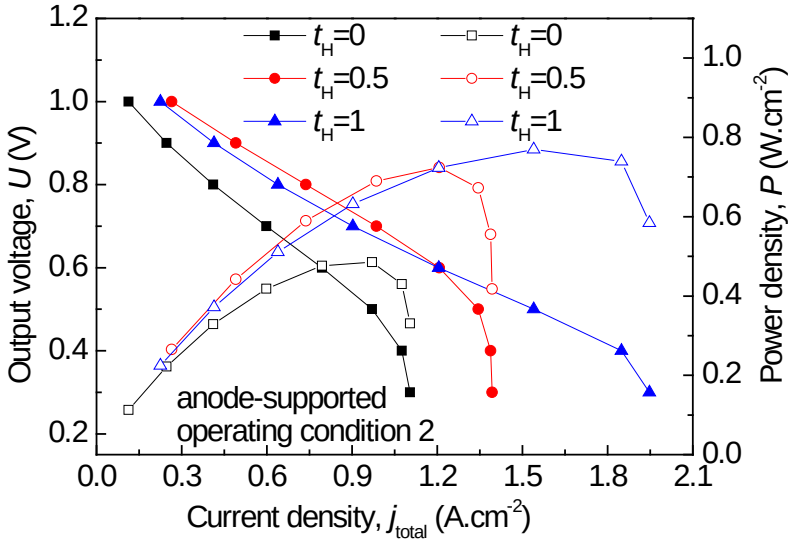

Fig. 5 Performance simulation of anode-supported SOFC in operating condition 2

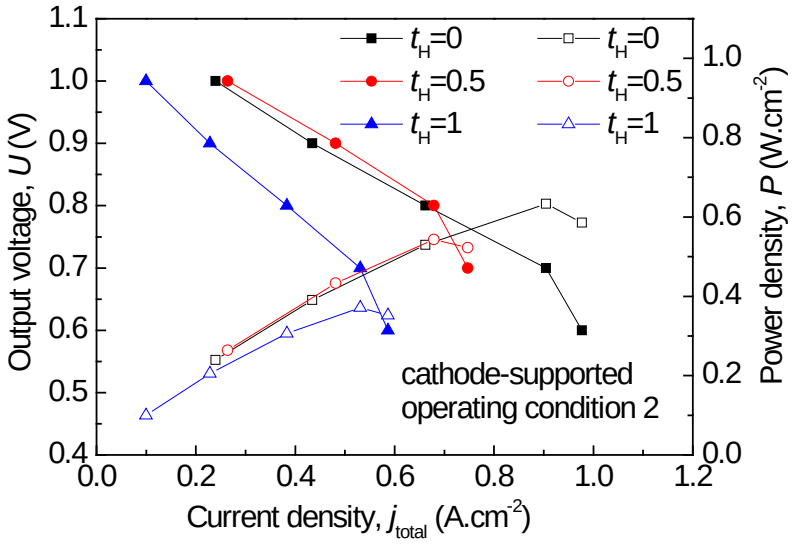

Fig. 6 Performance simulation of cathode-supported SOFC in operating condition 2

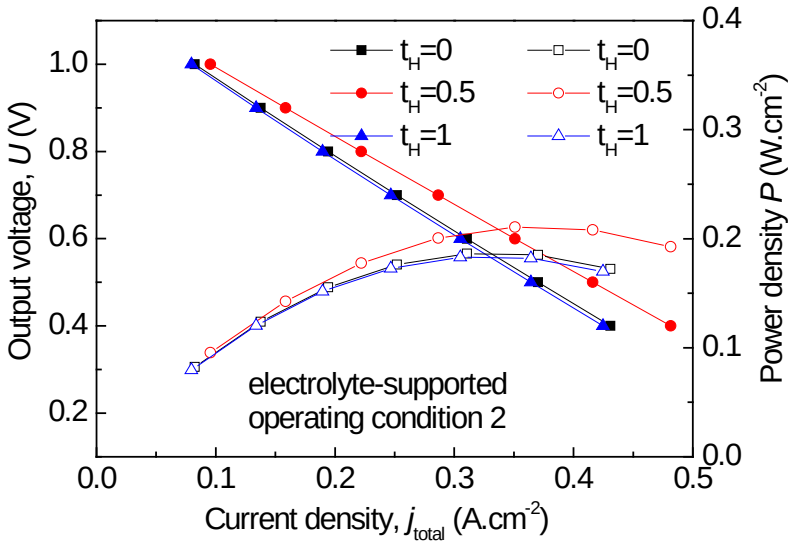

Fig. 7 Performance simulation of electrolyte-supported SOFC in operating condition 2

Simulations are performed to examine the effect of proton transfer number on the SOFC performance. Fig. 8 and Fig. 9 show variations of current density j_{total} with t_H at given output voltage U. For anode-supported SOFC in operating condition 1 (Fig. 8), the computed current density j_{total} increases with increasing t_H, reaches the maximum value at $t_H = 0.7$, and then decreases slightly with a further increase in t_H. For comparison, SOFCs with different

supporting structures in operating condition 2 are shown in Fig. 9. Similar to case 1, the maximum current density is found at a t_H value of 0.7 for anode-supported SOFC. For comparison, optimal t_H value of 0.2 is observed for cathode supported SOFC. The effect of t_H on performance of electrolyte-supported SOFC is small due to small thickness of the electrodes. The results are interesting as they demonstrate the feasibility of enhancing the SOFC performance by designing appropriate t_H value.

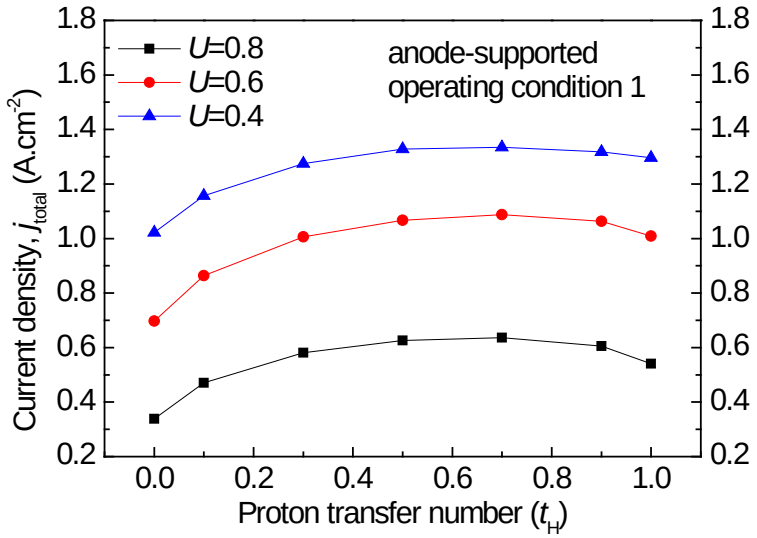

Fig. 8 Variation of current density j_{total} with different t_H in operating condition 1

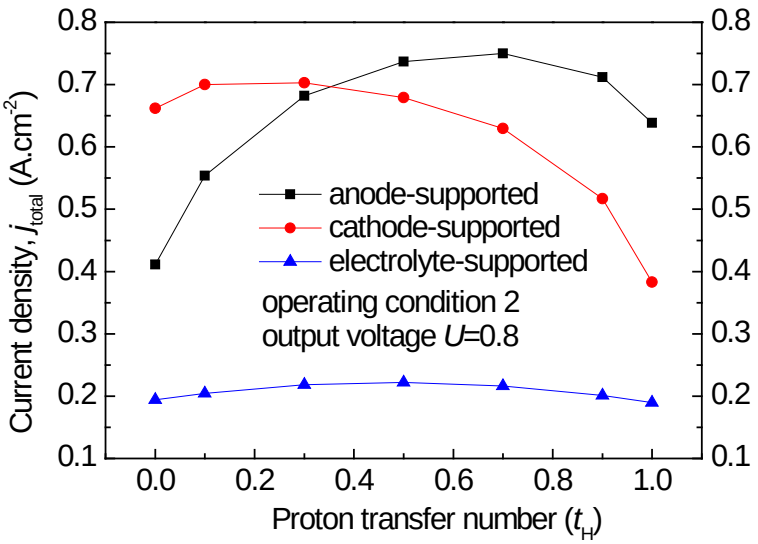

Fig. 9 Variation of current density j_{total} with different t_H in operating condition 2

3.2. Effect of co-ionic property on concentration overpotential in both electrodes

In a co-ionic conducting SOFC, the co-ionic property only affects the concentration overpotentials when the total conductivity of electrolyte is fixed. To gain a better understanding on the co-ionic effect on SOFC performance (shown in section 3.1), the concentration overpotentials in the electrodes are investigated in detail at various proton transfer number. As can be seen from Fig. 10, the difference between the anode and cathode concentration overpotentials is decreased with increasing proton transfer number (for operating condition 2).

Variation of concentration overpotential in each electrode with different t_H is shown in Fig. 11 and Fig. 12. For anode-support SOFC, the anode concentration overpotential decreases while the cathode concentration overpotential increases with increasing t_H from 0 to 1. As a result, the cathode concentration overpotential is higher than the anode concentration overpotential at $t_H = 1$. Variations of concentration overpotentials of cathode-supported SOFC and electrolyte-supported SOFC are also presented in Fig. 12. From the results presented in Figs. 11 and 12, it can be concluded that the difference between the anode concentration overpotential and cathode concentration overpotential can be reduced at certain t_H values.

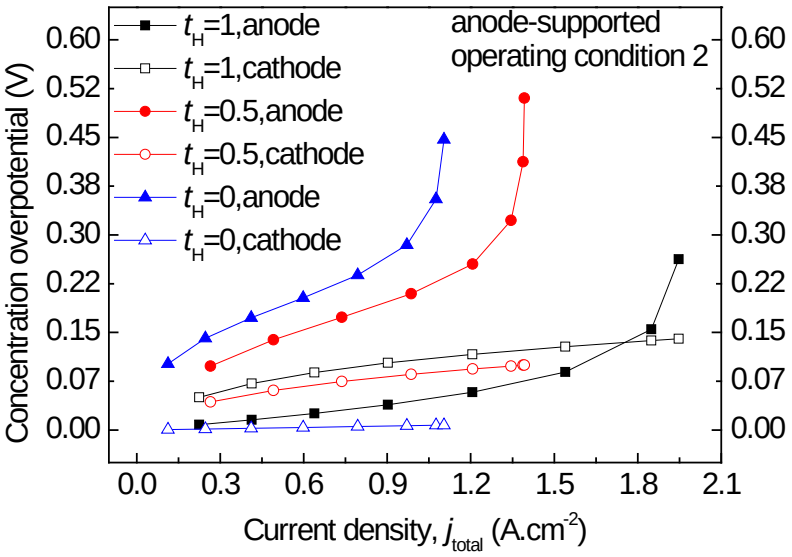

Fig. 10 Variation of concentration overpotential with different j_{total}

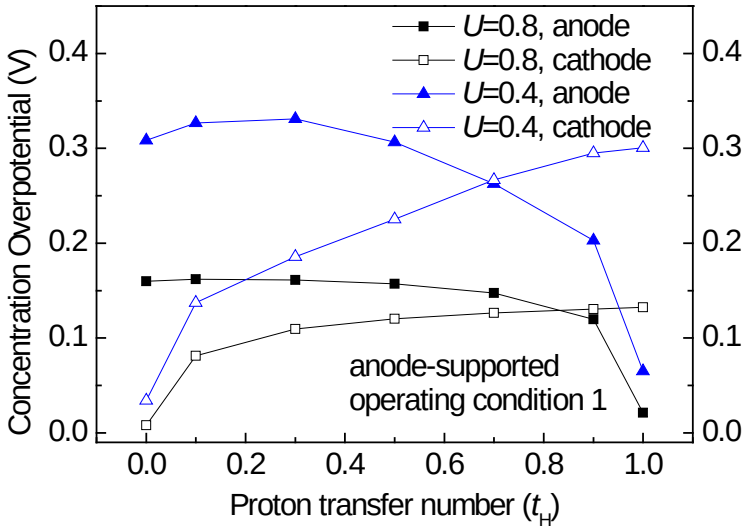

Fig. 11 Variation of concentration overpotential with different t_H in operating condition 1

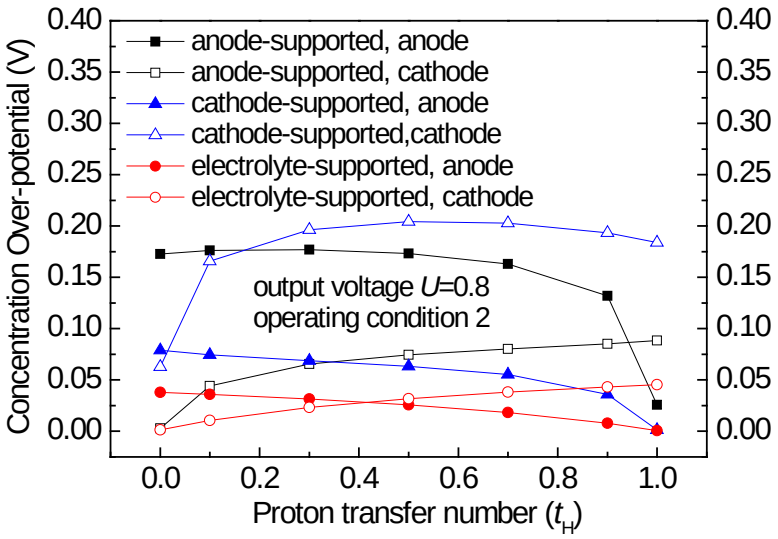

Fig. 12 Variation of concentration overpotential with different t_H in operating condition 2

4. Conclusion

In this paper, a new mathematical model for co-ionic conducting SOFC is established for actual performance analysis. Variations of Concentration overpotentials with different t_H and j_{total} are also studied. It can be concluded that, co-ionic conducting SOFC usually shows a better performance than H-SOFC (t_H=1) and O-SOFC (t_H=0) when current density j_{total} is not very large. In comparison with H-SOFC and O-SOFC, the co-ionic property reduces the concentration overpotential difference between anode and cathode at given proton transfer number. This study could improve our understanding for co-ionic conducting SOFC could help material selection for performance improvement.

Acknowledgement:

This research was supported by a grant (Project Number: PolyU 5238/11E) from Research Grant Council (RGC) of Hong Kong.

Reference

[1] Demin, A., Tsiakaras, P.: Thermodynamic analysis of a hydrogen fed solid oxide fuel cell based on a proton conductor, International Journal of Hydrogen Energy, vol. 26, no. 10, pp. 1103-1108 (2001).

[2] Iwahara, H.: Oxide-ionic and protonic conductors based on perovskite-type oxides and their possible applications, Solid State Ionics, vol. 52, no. 1–3, pp. 99-104 (1992).

[3] Iwahara, H.: High temperature protonic conductors and their applications, Solid State Ionics, pp. 575-586 (1992).

[4] Iwahara, H.: High temperature proton conducting oxides and their applications to solid electrolyte fuel cells and steam electrolyzer for hydrogen production, Solid State Ionics, vol. 28–30, Part 1, no. 0, pp. 573-578 (1998).

[5] Iwahara, H., Yajima, T., Hibino, T. & Ushida, H.: Performance of solid oxide fuel-cell using proton and oxide-ion mixed conductors based on Bace1-xsmxo3-Alpha, Journal of the Electrochemical Society, vol. 140, no. 6, pp. 1687-1691 (1993).

[6] Huang, J.B., Yuan, J.L., Mao, Z.Q. & Sunden, B.: Analysis and modeling of novel low temperature SOFC with a co-ionic conducting ceria based composite electrolyte, Journal of Fuel Cell Science and Technology, vol. 7, no. 1, 011-012 (2010).

[7] Bavarian, M., Kevrekidis, I.G. Benziger, J.B. & Soroush, M.: Modeling and bifurcation analysis of a coionic conducting solid oxide fuel cell, Industrial & Engineering Chemistry Research, vol. 52, no. 9, pp. 3165-3177 (2013).

[8] Demin, A., Tsiakaras, P., Gorbova, E. & Hramova, S.: A SOFC based on a co-ionic electrolyte, Journal of Power Sources, vol. 131, no. 1–2, pp. 231-236 (2004).

[9] Demin, A., Gorbova, E. & Tsiakaras, P.: High temperature electrolyzer based on solid oxide co-ionic electrolyte: A theoretical model, Journal of Power Sources, vol. 171, no. 1, pp. 205-211 (2007).

[10] Ni, M., Leung, M.K.H. & Leung, D.Y.C.: Parametric study of solid oxide fuel cell performance, Energy Conversion and Management, vol. 48, no. 5, pp. 1525-1535 (2007).

[11] Hernández-Pacheco, E., Singh, D., Hutton, P.N., Patel, N. & Mann, M.D.: A macro-level model for determining the performance characteristics of solid oxide fuel cells, Journal of Power Sources, vol. 138, no. 1–2, pp. 174-186 (2004).

[12] Suwanwarangkul, R., Croiset, E., Fowler, M.W., Douglas, P.L., Entchev, E. & Douglas, M.A.: Performance comparison of Fick's, dusty-gas and Stefan–Maxwell models to predict the concentration overpotential of a SOFC anode, Journal of Power Sources, vol. 122, no. 1, pp. 9-18 (2003).

[13] Ni, M., Leung, M.K.H. & Leung, D.Y.C.: Theoretical analysis of reversible solid oxide fuel cell based on proton-conducting electrolyte, Journal of Power Sources, vol. 177, no. 2, pp. 369-375 (2008).

[14] Peng, R.R., Wu Y., Yang, L.Z. & Mao, Z.Q.: Electrochemical properties of intermediate-temperature SOFCs based on proton conducting Sm-doped BaCeO3 electrolyte thin film, Solid State Ionics, vol. 177, no. 3–4, pp. 389-393 (2006).

[15] Ni, M., Leung, M.K.H. & Leung, D.Y.C.: Mathematical modeling of proton-conducting solid oxide fuel cells and comparison with oxygen-ion-conducting counterpart, Fuel Cells, vol. 7, no. 4, pp. 269-278 (2007).

Appendix. 1

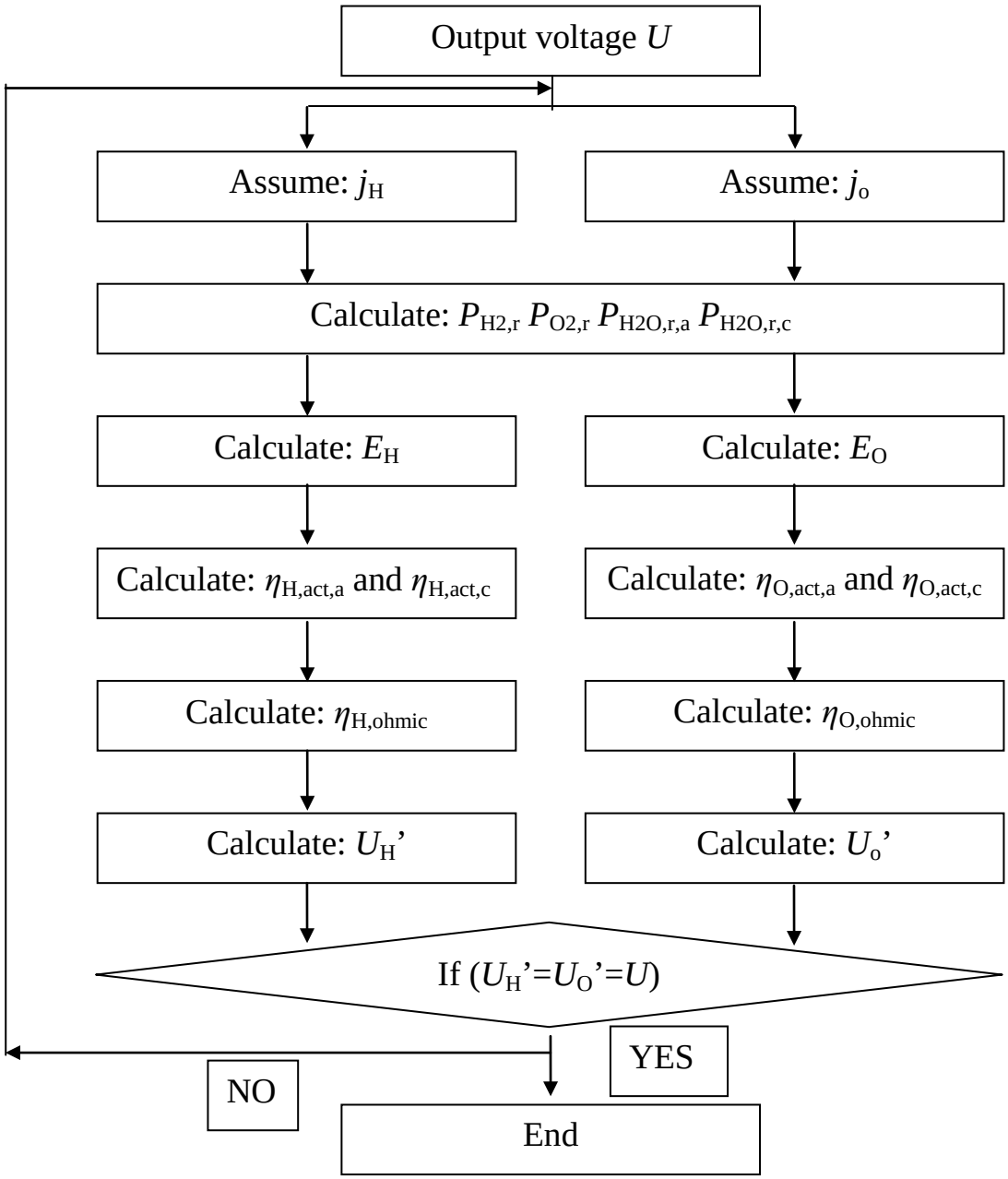
Output voltage U
Assume: j_H
Assume: j_o
Calculate: $P_{H2,r}$ $P_{O2,r}$ $P_{H2O,r,a}$ $P_{H2O,r,c}$
Calculate: E_H
Calculate: E_O
Calculate: $\eta_{H,act,a}$ and $\eta_{H,act,c}$
Calculate: $\eta_{O,act,a}$ and $\eta_{O,act,c}$
Calculate: $\eta_{H,ohmic}$
Calculate: $\eta_{O,ohmic}$
Calculate: U_H'
Calculate: U_o'
If (U_H'=U_O'=U)
YES
NO
End